Received: 2 May 2023 | Accepted: 19 July 2023

DOI: 10.1111/cen.14955

REVIEW ARTICLE

WILEY

Paediatric phaeochromocytoma and paraganglioma: A clinical update

Matthew A. Nazari[1] | Abhishek Jha[1] | Mickey J. M. Kuo[1,2] | Mayank Patel[1] | Tamara Prodanov[1] | Jared S. Rosenblum[1] | Sara Talvacchio[1] | Alberta Derkyi[1] | Kailah Charles[1] | Karel Pacak[1]

[1]Developmental Endocrinology, Metabolism, Genetics and Endocrine Oncology Affinity Group, Section on Medical Neuroendocrinology, Eunice Kennedy Shriver National Institute of Child Health and Human Development, National Institutes of Health, Bethesda, Maryland, USA

[2]Medical Genetics Branch, National Human Genome Research Institute, National Institutes of Health, Bethesda, Maryland, USA

Correspondence
Karel Pacak, Developmental Endocrinology, Metabolism, Genetics, and Endocrine Oncology Affinity Group, Section on Medical Neuroendocrinology, *Eunice Kennedy Shriver* National Institute of Child Health and Human Development, National Institutes of Health, Bldg 10, CRC, Room 1E-3140, 10 Center Dr MSC-1109, Bethesda, MD 20892-1109, USA.
Email: karel@mail.nih.gov

Funding information
Intramural Research Programme of the National Institutes of Health, Eunice Kennedy Shriver National Institute of Child Health and Human Development; Intramural Research Programme of the Center for Cancer Research, National Cancer Institute

Abstract

Paediatric phaeochromocytomas and paragangliomas (PPGLs), though rare tumours, are associated with significant disability and death in the most vulnerable of patients early in their lives. However, unlike cryptogenic and insidious disease states, the clinical presentation of paediatric patients with PPGLs can be rather overt, allowing early diagnosis, granted that salient findings are recognized. Additionally, with prompt and effective intervention, prognosis is favourable if timely intervention is implemented. For this reason, this review focuses on four exemplary paediatric cases, succinctly emphasizing the now state-of-the-art concepts in paediatric PPGL management.

KEYWORDS
disease management, genetics, molecular imaging, paediatric, paraganglioma, pathology, phaeochromocytoma

1 | INTRODUCTION

The chromaffin cell tumours phaeochromocytoma and paraganglioma (PCC, PGL, collectively PPGL) produce and release catecholamines. Although paediatric PPGLs are a rare entity (estimated incidence: 1–2 per 1,000,000 person-years), they are nevertheless associated with substantial morbidity and mortality if unrecognized; thus, the gravity of prompt recognition and effective management cannot be overstated.[1–5] Paediatric PPGL patients are frequently symptomatic (64%–93%; with headaches: 39%–95%; diaphoresis: 90%; and palpitations: 53%) and hypertensive (about 90%), with an underlying heritable syndrome (about 80%) and initially present with advanced (multifocal/metastatic) disease (up to 62%), often permitting a rapid diagnosis once key features are recognized.[6–11] Given the rarity of paediatric PPGL and the grave importance of this disease, we herein provide four illustrative paediatric cases. Paediatric PPGLs are often heritable and rely heavily upon a pathologic diagnosis and functional imaging for evaluation, while also, usually, mandating surgical resection as the gold standard for treatment. As such, these cases will showcase up-to-date concepts in histopathology, genetics, imaging, and perioperative management.

2 | CASE 1: HISTOPATHOLOGY

A healthy 13-year-old male with a positive paternal history tested positive for the same *SDHB* pathogenic variant. Though he was asymptomatic with negative biochemical testing, conventional imaging studies (computed tomography [CT]/magnetic resonance imaging

[MRI]) revealed a tumour located on the anterior dome of the bladder, which was subsequently avid on ^{68}Ga-DOTA(0)-Tyr(3)-octreotate (^{68}Ga-DOTATATE) positron-emission tomography/CT (PET/CT) and ^{18}F-fluorodeoxyglucose (^{18}F-FDG) PET/CT. Surgical resection was planned.

During the operation, a consultation was requested to confirm margin-free adjacent tissue to the bladder wall upon tumour resection (1A). Gross dissection revealed a 2 × 2 × 1 cm sample with a tumour measuring 0.8 × 0.7 × 0.6 cm (1B) brown-tan in colour (upon bisection) and glistening pink-tan bladder mucosa.

Haematoxylin and eosin (H&E) staining of the tumour demonstrated cells—with round hyperchromatic nuclei and stippled chromatin—arranged in nests with intervening fibrovascular septa (Figure 1; 1C). Subsequent immunohistochemical stain demonstrated granular cytoplasmic positivity with chromogranin A staining (Figure 2A), diffuse cytoplasmic positivity with synaptophysin staining (Figure 2B), net-like sustentacular cells highlighted by S100 staining (Figure 2C), and a Ki-67 index of less than 1% (Figure 2D; 1D). *SDHB* staining was negative in tumour cells and positive in adjacent cells (Figure 3; 1E). Pankeratin staining with cytokeratin AE1/AE3 and CAM 5.2 were negative (1F). Further testing was unnecessary and therefore omitted (2G). Taken together, these findings are consistent with a PGL and negative for urothelial carcinoma.

Key learning points

- *1A*: Endeavour for negative tumour margins when resecting PPGLs. Although not statistically significant ($p = .713$), macroscopically positive margins upon PPGL resection are associated with far less overall survival time (90 months) compared to completely negative surgical margins (143 months), while negative margins are associated with low recurrence rates (3.6%–5.1% local recurrence; median duration: 70 months).[12,13]
- *1B*: The size of the primary tumour correlates with risk of metastasis and 5-year survival; this is especially true for *SDHB*-mutated PPGLs.[14] Metastasis amongst *SDHx*-mutated tumours is heterogenous (*SDHA*: 0%–14%; *SDHC*: rarely metastatic; *SDHD*: <5%), with *SDHB* being the most metastatic (34%–71% metastasis) with 36% 5-year survival.[15–17] In *SDHB*-mutated PPGLs, a primary tumour ≥4.5 cm is associated with earlier metastasis ($p = .003$) and tumours >5.5 cm are associated with worse survival ($p = .008$).[14]
- *1C*: H&E staining is adequate for recognizing key features of PPGLs, thus allowing for a rapid preliminary diagnosis. Hallmark features on H&E staining include nested architecture ("*Zellballen*") and "salt and pepper" chromatin patterns. Request chromogranin (1), synaptophysin (2), and S100 (3) staining for suspected PPGLs as these are the three (1–3) important immunohistochemical stains used to confirm the diagnosis.
- *1D*: Ki-67 index is often, although not always, a useful proliferative index associated with metastasis. Previous studies have shown nonmetastatic PPGLs to have a Ki-67 index of approximately 1%–2% with metastatic PPGLs having a Ki-67 index of approximately 4.5%–10% ($p < .001$).[18] Here, the Ki-67 index (Figure 2D) was <1% in this patient with nonmetastatic disease.
- *1E*: If suspicious features are present, such as a positive family history, a PGL, and young age, as in this patient, perform SDHB immunostaining on the tumour. As a tumour suppressor gene, subsequent staining, accordingly, revealed absent SDHB (Figure 3). *SDHB* staining can rapidly be performed, thus expediting a preliminary molecular diagnosis in familial and other cases (vs. send-out genetic testing).[3,19]
- *1F*: PGLs are rare; therefore, more common and anatomically likely cancers (here, urothelial carcinoma) should be considered. Pankeratin staining was performed using the combination of cytokeratin

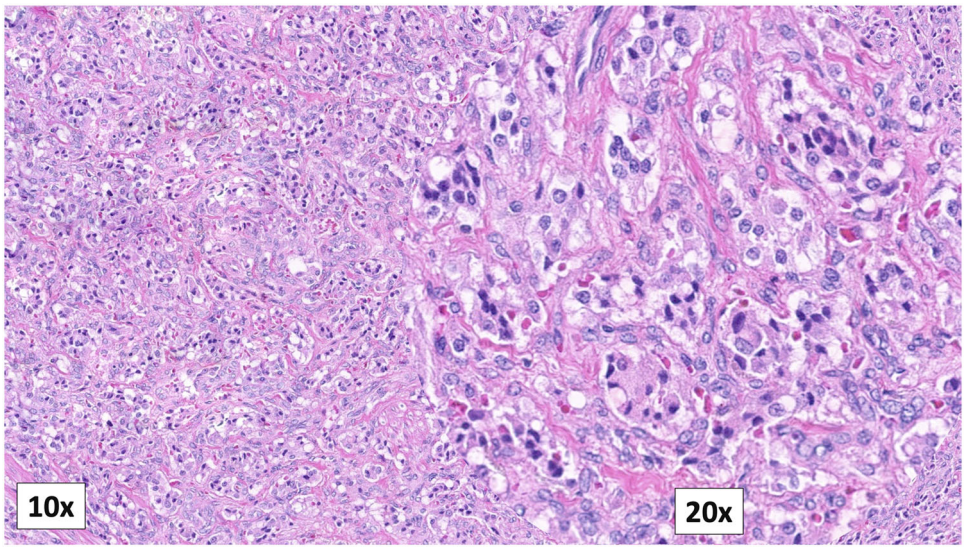

FIGURE 1 Bladder tumour was stained with haematoxylin and eosin shown here at ×10 magnification displaying a nested architecture with intervening fibrovascular septa. The inlet image in the figure is magnified to ×20 showing round nuclei with varying patterns of both hyperchromatic and stippled chromatin.

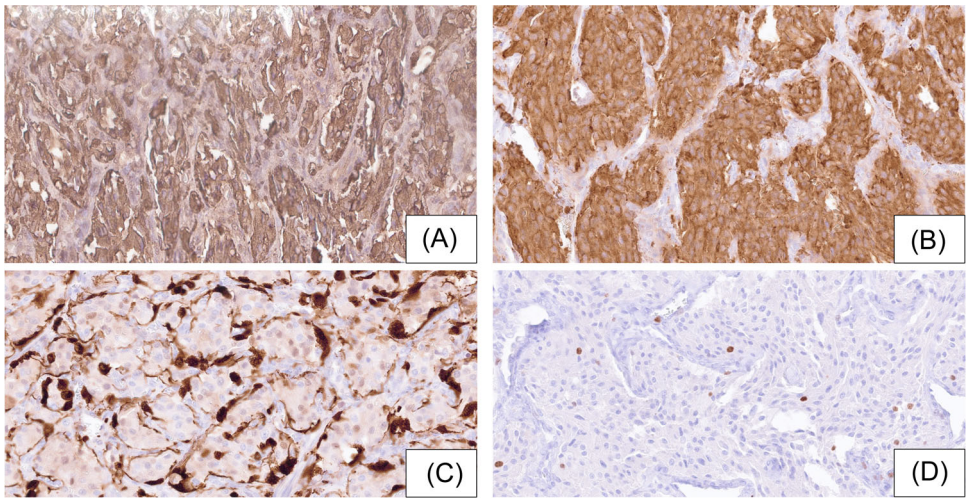

FIGURE 2 The figure includes four (A–D) immunostains performed on the bladder tumour. (A) Chromogranin staining shows granular cytoplasmic positivity in the tumour cells. (B) Synaptophysin shows diffuse cytoplasmic positivity in the tumour cells. (C) S100 staining shows the supportive sustentacular cells staining positive with the tumour cells staining negative. (D) Ki-67 is shown in a region with the highest staining at ×20. Note less than 1% of the tumour cell nuclei stained positive with Ki-67.

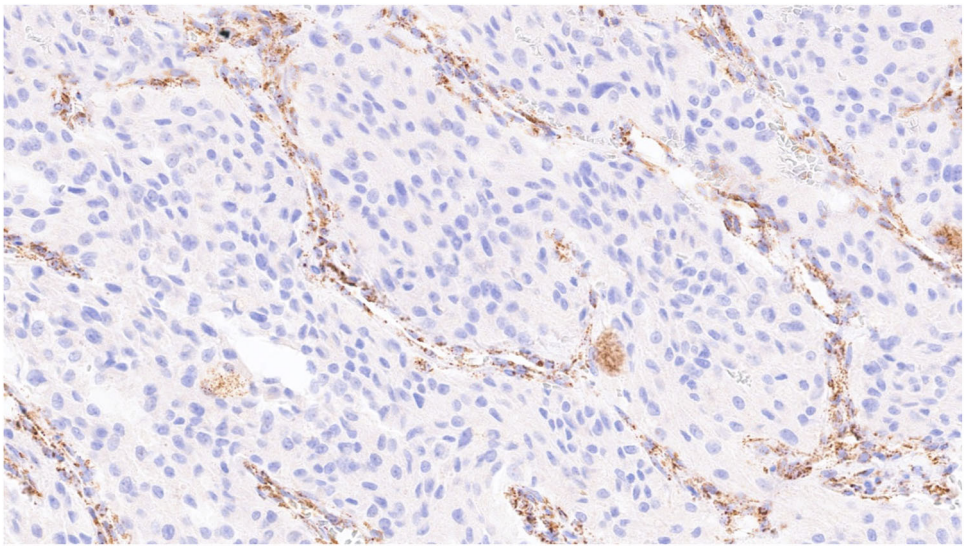

FIGURE 3 *SDHB* staining is lost in the tumour cells but retained in the cells of the intervening septa.

AE1/AE3 and CAM 5.2, both of which showed immunonegativity in the tumour cells, excluding urothelial carcinoma.

- *1G*: The best diagnostic approach should omit costly and unnecessary studies. A summary of immunohistochemical stains and their findings in PPGL are tabulated in Table 1.

3 | CASE 2: GENETICS

A 20-year-old female presented to the Emergency Department with abdominal pain and was incidentally found to have a 3.8 cm right adrenal mass on abdominopelvic CT suspicious for a PCC. Subsequent biochemical testing demonstrated elevated plasma normetanephrine (approximately 12 times the upper reference limit, URL) and normal plasma metanephrine with positive uptake in a right adrenal mass on ^{18}F-fluorodopa (^{18}F-FDOPA) PET/CT. She was started on prazosin and referred for surgical intervention.

Subsequent right adrenalectomy was performed and germline testing (2A) from peripheral blood was negative, while somatic testing of the tumour itself (2B) was positive for a pathogenic variant in *VHL* c.238A > G (p.Ser80Gly, 2C) at 33% variant allele frequency. The patient was then lost to follow-up precluding the opportunity for further genetic counselling and screening (for other abnormalities associated with *VHL* pathogenic variants [2D]).

TABLE 1 Summary of immunohistochemical stains utilized in the diagnosis of phaeochromocytoma and paraganglioma (PPGL).

Immunohistochemical stain	Staining pattern in PPGL
Chromogranin	Cytoplasmic granular positivity
Synaptophysin	Cytoplasmic diffuse positivity
S100	Positive in sustentacular cells (negative in tumour cells)
INSM-1	Nuclear positivity
Ki-67	Positive in actively proliferating cells
GATA-3	Variable positivity but nonspecific
SDHB	Negativity in tumour cells signifies *SDHB* protein loss

Key learning points

- *2A*: PPGLs are the most heritable tumour with over 27 known susceptibility genes; therefore, genetic testing, even in the absence of family history, should be performed in all patients.[20–22] Notably, 70%–84% of paediatric PPGL patients have a known causal pathogenic variant, most commonly in the *VHL* gene (*VHL*, 27%–51%) and the succinate dehydrogenase subunit genes (collectively referred to as *SDHx*, 13%–39% in *SDHB* and 8%–10% in *SDHD*) and less often in the ret proto-oncogene (*RET*, causing multiple endocrine neoplasia type 2, MEN-2, 0.6%–10%) and neurofibromin 1 gene (*NF1*, causing neurofibromatosis type 1 or NF1, 1%).[5–8,10,11,23–26]
- *2B*: Paediatric PPGL patients should receive genetic counselling and consideration of both germline (e.g., blood, buccal swab, or saliva) and somatic genetic testing (tumour tissue itself). This is because about 30%–40% of genetic variants in PPGLs are somatic, not germline.[20] Next-generation sequencing, including exome sequencing, should be strongly considered if a genetic driver variant is not initially identified, recognizing the extensive genetic nature of these tumours.[22]
- *2C*: Note that *VHL*-mutated tumours have prototypical findings such as a noradrenergic biochemical phenotype (producing predominantly norepinephrine) in contrast to *RET*-mutated tumours (MEN-2) with an adrenergic biochemical phenotype.[27] Further, a salient feature of VHL tumours is avid uptake on ^{18}F-DOPA PET/CT. Finally, it is also important to recognize that if a genetic variant such as *VHL* is identified beyond tumour tissue (e.g., a mosaic or germline variant), just like in MEN-2 and NF1, then patients should be screened for associated syndromic abnormalities (such as hemangioblastomas in the brain and/or eyes or renal cell carcinoma in patients with VHL syndrome).[28]
- *2D*: Given the high frequency of causal genetic variants found in PPGL, genetic counsellors and medical geneticists are essential members of a multidisciplinary team as they can aid in discussing the implications of genetic findings to patients/parents and inform aspects of management (such as screening for associated abnormalities).[29,30]

4 | CASE 3: IMAGING

A 15-year-old male with a history of autism spectrum disorder with global developmental delay and multiple secretory PGLs with a known *SDHB* pathogenic variant was referred to our institution. Upon evaluation, he had an elevated plasma norepinephrine (3.4× URL), normetanephrine (13.4× URL), and chromogranin A (8.5× URL). Whole-body CT, ^{18}F-FDOPA, and ^{18}F-FDG PET/CT revealed a 3.8 × 3.6 cm right carotid body PGL (Figure 4A–D, red arrows), a left periaortic PGL (Figure 4A–D, green arrows), and multiple bone metastases (3A). Initial ^{68}Ga-DOTATATE PET/CT was omitted as it was unavailable at our institute at the time of the evaluation (3B).

The patient subsequently underwent a right carotid artery occlusion test and embolization followed by palliative surgical resection of the right carotid body PGL as this lesion was causing compressive symptoms. Re-evaluation 1.5 years later demonstrated an elevated plasma norepinephrine (1.2× URL), normetanephrine (2.5× URL), chromogranin A (2.0× URL), and 3-methoxytramine (1.9× URL). Imaging studies with whole-body CT, ^{68}Ga-DOTATATE PET/CT, ^{18}F-FDOPA PET/CT, and ^{18}F-FDG PET/CT revealed a 3.5 × 2.5 cm recurrent/residual tumour in the right neck region (Figure 4E–G, red arrows) and a 1.7 × 1.5 cm left periaortic PGL (Figure 4E–G, green arrows; 3C). ^{68}Ga-DOTATATE PET/CT revealed bone lesions (Figure 4E, blue arrows) that were not noted on ^{18}F-FDOPA PET/CT (Figure 4F) or ^{18}F-FDG PET/CT (Figure 4G; 3D). An interval increase in bone metastases was noted and ^{123}I-metaiodobenzylguanidine (^{123}I-MIBG) scintigraphy was obtained to determine the suitability of ^{123}I-MIBG therapy (3E). Unfortunately, the patient was lost to follow-up.

Key learning points

- *3A*: Both anatomic (CT/MRI) and functional (various PET scans) imaging must be performed in PPGL patients. Functional imaging modalities, however, are indispensable in evaluating, monitoring, and treating these patients and rely upon radiopharmaceuticals that bind to/enter PPGLs with greater specificity, providing an exceptional characterization of tumours. These radiopharmaceuticals include conjugated radiolabeled somatostatin analogues (^{68}Ga-DOTATATE, binding somatostatin type 2 receptors), ^{18}F-FDOPA (entering via the L-type amino acid transporter 1), the norepinephrine analogue ^{123}I-MIBG (entering via norepinephrine transporters), and ^{18}F-FDG (radiolabeled glucose entering via glucose transporters), a nonspecific oncologic radiopharmaceutical.[31–33] Often, functional imaging with ^{68}Ga-DOTATATE or ^{18}F-FDOPA PET/CT is able to locate tumours in unusual locations (e.g., cardiac paragangliomas), which are not localized by anatomic imaging.[34] ^{64}Cu-DOTATATE PET/CT is an alternative to ^{68}Ga-DOTATATE PET/CT, which performs similarly to ^{68}Ga-DOTATATE based on initial results in PPGL.[35]
- *3B*: Whole-body CT/MRI and ^{68}Ga/^{64}Cu-DOTATATE PET provide the best initial imaging approach for metastatic paediatric PPGL.[36] ^{68}Ga-DOTATATE had superior per-lesion sensitivity (93.5%) compared to ^{18}F-FDG (79.4%), and CT/MRI (73.8%) in the detection of metastatic PPGLs, except for abdominal lesions

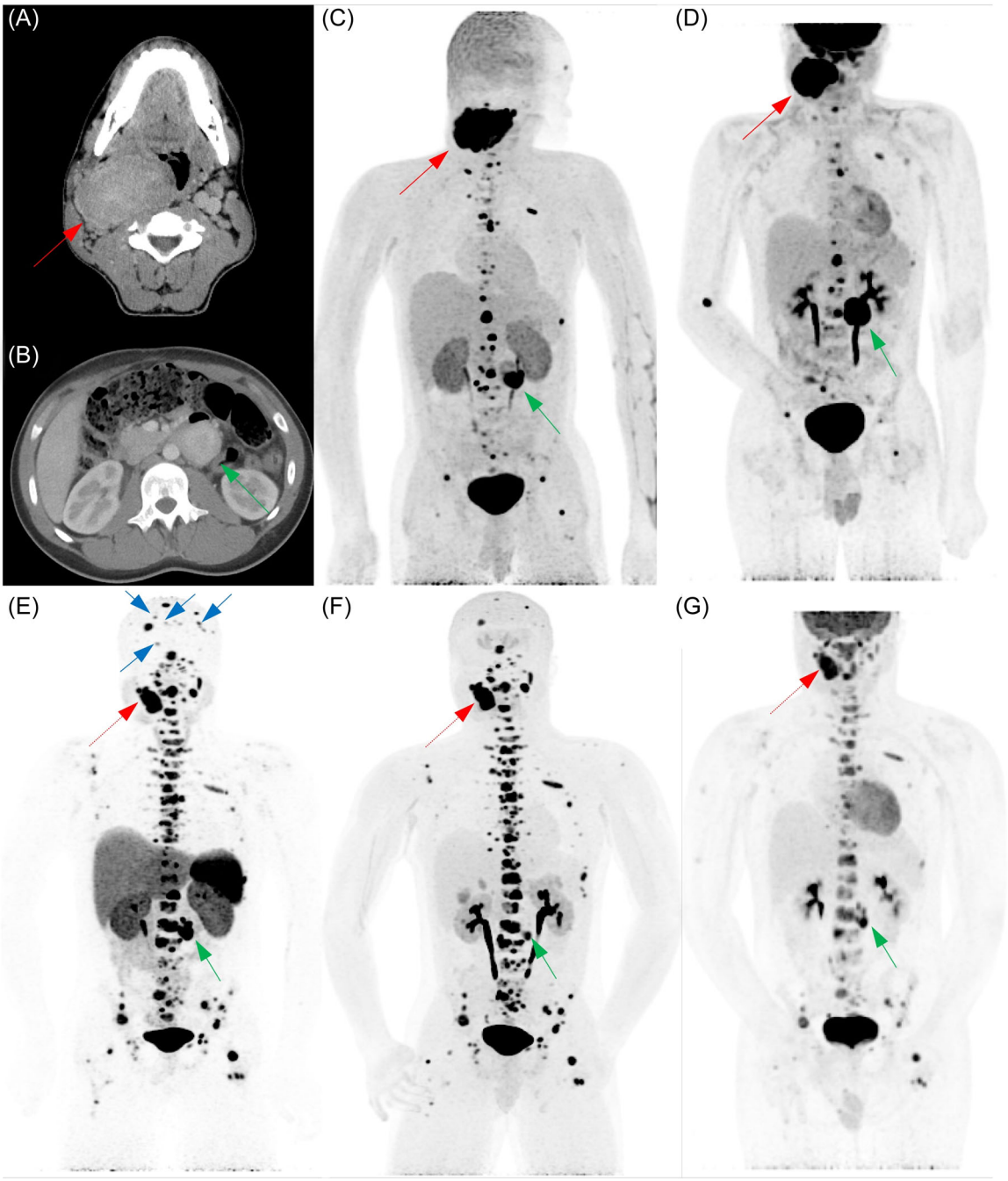

FIGURE 4 The axial computed tomography (CT) (A, B) images and maximum intensity projection images of ^{18}F-fluorodopa. ^{18}F-fluorodeoxyglucose images from the initial visit reveal a 6.8 × 3.8 cm right carotid body PGL (red arrow, A, C, and D) and a 3.8 × 3.6 cm left periaortic PGL (green arrow, B–D) along with multiple bone metastases (C, D). The patient subsequently underwent right carotid body tumour resection, which was proven to be a PGL on histopathology. Follow-up imaging (E–G) after 1.5 years with ^{68}Ga-DOTA(0)-Tyr(3)-octreotate (^{68}Ga-DOTATATE) (E), ^{18}F-fluorodopa (F), and ^{18}F-fluordeoxyglucose (G) demonstrate a 3.5 × 2.5 cm recurrent/residual tumour in the right carotid body region (red arrows, E–G) and a significantly smaller left periaortic PGL (green arrows, E–G). Further, the number of bone metastases has increased (size and number) compared to the initial evaluation. On subsequent evaluation, ^{68}Ga-DOTATATE (E) was found to be the superior radiopharmaceutical as it detected additional small bone metastases (a few are shown by the blue arrows in panel E).

outside the liver and adrenal glands (best characterized by ^{18}F-FDG PET/CT).[36]

- *3C*: Obtain biochemical evaluation with plasma metanephrines, anatomic imaging with CT or MRI, and functional imaging with ^{68}Ga/^{64}Cu-DOTATATE PET/CT 3–6 months postoperatively. Importantly, although CT and MRI can be complementary, clinical circumstances should dictate the best overall decision across practice settings.[37] CT is better for visualizing lung lesions and can be

performed rapidly, often obviating the need for sedation; this benefit is offset by radiation exposure.[37] MRI better visualizes liver and bone lesions and avoids radiation exposure, but is more expensive and requires longer scanning times, which may necessitate sedation.[5,38]

- *3D*: Serial re-evaluation ("follow-up") in patients with PPGLs must be tailored to tumour location and/or underlying genetic profile and should utilize functional imaging scans. The following functional imaging radiopharmaceuticals are the preferred choices based on the most recent nuclear medicine society guidelines and recent research:
  - ^{68}Ga-DOTATATE: Cluster 1A genes (especially *SDHx*), unknown pathogenic variants, head and neck, metastatic, and metastatic paediatric *SDHx* PPGL.[31,32,36,39–43]
  - ^{18}F-FDOPA and ^{123}I-MIBG scintigraphy: Cluster 1B and 2 genes.[31,42,44,45]
  - ^{18}F-FDOPA: Apparently sporadic PCC.[46]
- *3E*: Obtaining ^{68}Ga/^{64}Cu-DOTATATE PET/CT and ^{123}I-MIBG scintigraphy can directly inform targeted radiotherapy as the same radiotracer used to image these tumours can be used to deliver targeted radiation with ^{177}Lu-DOTATATE and high- or low-specific activity ^{123}I-MIBG respectively.[47,48]

5 | CASE 4: PERIOPERATIVE MANAGEMENT

A 12-year-old male with a paternally inherited *VHL* pathogenic variant was found to have elevated urine metanephrines. Subsequent abdominopelvic CT found bilateral adrenal masses (right: 3.9 × 3.5 × 5.5 cm; left: 2.1 × 2.3 × 3.2 cm) and ^{68}Ga-DOTATATE PET/CT exhibited bilateral adrenal avidity. Findings were consistent with PCC. The patient was evaluated in our clinic and planned for a future bilateral partial adrenalectomy.

Two weeks preceding admission, the patient's blood pressure and heart rate ranged from 99 to 120/62–78 mmHg (4A) and 84–129 beats per minute, respectively. Doxazosin 1 mg daily was started (4B). Upon admission 7 days before the operation, repeat biochemical testing demonstrated elevated plasma 3-methoxytyramine, chromogranin A, norepinephrine and normetanephrine (4C). Five days before the patient's operation, the blood pressure remained elevated and an echocardiogram was obtained. Doxazosin was increased to 1 mg twice daily and maintenance fluids (73 mL/h for a weight of 33 kg) were started while encouraging oral hydration and a diet high in sodium (4D). The echocardiogram did not demonstrate chamber dilation or hypertrophy and biventricular systolic and diastolic function were grossly intact (4E). Two days before the operation, atenolol 12.5 mg twice daily was added for sinus tachycardia (heart rates of 100–112 beats per minute). The day before the operation, maintenance fluids were increased by 25% (to 91 mL/h). The morning of the operation, the blood pressure was 99/50 mmHg and the heart rate was 79 beats per minute. Doxazosin was given, atenolol was held (4F), and 25 mg of oral hydrocortisone was given (4G). Intraoperatively, the patient was given 1600 mL of intravenous (IV) crystalloid, 50 mg of IV hydrocortisone and two 0.1 mg/kg boluses of IV nicardipine (4H).

Postoperatively, the patient's blood pressures remained stable on 50 mL/h of IV crystalloid, and 25 mg of hydrocortisone was given daily until a cosyntropin (120 µg) stimulation test was performed, with cortisol levels of 10.2, 14.5 and 15.6 at 0, 30 and 60 min after cosyntropin administration, at which point the patient was transitioned to 10 mg of hydrocortisone in the morning and 5 mg of hydrocortisone in the afternoon. The patient has subsequently been followed closely by endocrinological surgery and the dose has been tapered with plans for eventual cessation.

Key learning points

- *4A*: Use age-specific blood pressure percentiles in paediatric patients <13 years old. Prompt treatment should be provided for patients with stage II hypertension (systolic BP ≥95th percentile + 12 mmHg or ≥140/90 mmHg, whichever is lower), and we prefer to treat patients so that their goal BP is <90th percentile.[49]
- *4B*: α-Adrenoceptor blockade should precede β-adrenoceptor blockade. This is because blocking β_2-adrenoceptor-mediated vasodilation can allow for unopposed α_1-adrenoceptor-mediated vasoconstriction, worsening hypertension.[50] For this same reason, beware of IV labetalol as monotherapy in paediatric patients with PPGL as it provides 1:7 α:β-adrenoceptor blockade, thus precipitating hypertension.[51]
- *4C*: The metabolites of catecholamines are used to screen for PPGL with an elevation of >2× URL being concerning for a PPGL. Age-adjusted cutoffs must be used for normetanephrine (a metabolite of norepinephrine), and the following equation: $(2.07 \times 10^{-6} \times \text{age}^3) + 0.545$ can approximate the URL in nmol/L. Note 3-methoxytyramine (a metabolite of dopamine) and metanephrine (a metabolite of epinephrine) have a URL of 0.10 and 0.45 nmol/L and do not need to be adjusted for age.[52]
- *4D*: Patients with PPGLs have reduced intravascular volume. Immense α_1-adrenoceptor-mediated vasoconstriction leads to (1) extravasation of fluid out of the vascular space and (2) pressure natriuresis.[53,54] Consequently, PPGL patients have an approximate 15% decrease in intravascular volume, or about 500 mL in the average person.[55] Thus, when giving vasodilating (e.g., α-adrenoceptor-blocking) agents, hypotension can occur as the vascular space expands, while the remaining intravascular volume is often insufficient.[56] It is, therefore, prudent to begin hydration and salt intake when initiating α-adrenoceptor-blocking agents or when removing a PPGL to avoid/mitigate this hypotension.[57]
- *4E*: Consider obtaining echocardiograms in PPGL patients. Hypertension- and/or catecholamine-induced myocardial remodelling can occur in PPGL patients, compromising proper myocardial function.[58] An important example of acute cardiomyopathy is 'stress' or 'Takotsubo-like' cardiomyopathy (seen in 1.4%–5.6% of adult PPGL patients), whereby myocardial contraction is regionally suppressed but in the absence of a causative coronary occlusion.[59–61] Therefore, obtain an echocardiogram in PPGL patients with a history of hypertension, signs/symptoms of heart failure, or rapid reduction in blood pressure.[51]

- *4F*: Calibrate preoperative adrenoceptor blockade to clinical circumstances. Accordingly, obtain a heart rate and blood pressure 1–2 h preoperatively. In patients who are hypertensive and tachycardic, provide both α- and β-adrenoceptor blockade. In patients otherwise without hypertension or tachycardia, consider the impact of administering immediate preoperative blockade on intra-/postoperative hemodynamic stability and hold blockade if patients are hypotensive or bradycardic to avoid postoperative 'overshoot'.
- *4G*: Intraoperative and immediate postoperative hypotension is commonly due to (1) a relative decrease in intravascular volume (see 4D), (2) bleeding or (3) adrenal insufficiency in patients with adrenal procedures, and less often due to (4) suppression of myocardial contractile force (see 4E) or (5) a condition leading to obstructive shock (pulmonary embolism, abdominal compartment syndrome, etc., depending on the surgery).[57,62] Patients undergoing adrenal procedures (here a partial adrenalectomy) are at risk of postoperative adrenal insufficiency; thus, IV hydrocortisone is provided before anaesthesia induction (usually 50–100 mg) and then treated with IV hydrocortisone every 8 h (doses vary between 50 and 100 mg).[62,63] Taper over the next 24–48 h transitioning to oral hydrocortisone (10–12 mg × body surface area in mg/m^2) if the patient can tolerate oral medications and if the postoperative course is otherwise uneventful without additional physiologic stressors.[62,63] Then, consider cosyntropin stimulation testing 48–72 h after the operation as this informs ongoing dosing/management.[62]
- *4H*: Calcium channel blockers are valuable adjunctive agents when acutely treating catecholamine-induced hypertension and sinus tachycardia. These agents may be added to or in some cases may be used in place of adrenoceptor-blocking agents.[51,64] We use oral amlodipine (1–5 years old: 0.1–0.6 mg/kg/dose up to twice daily, maximum daily dose: 5 mg/day; >5 years old: 2.5–10 mg/day) or oral nifedipine (0.2–0.3 mg/kg/dose up to three times a day) for catecholamine-induced hypertension, diltiazem (0.5 mg/kg/dose up to four times a day, maximum dose 3.5 mg/kg/day) for catecholamine-induced sinus tachycardia, and oral verapamil (2–3 mg/kg/dose up to three times a day, maximum dose 480 mg/day) when both hypertension and sinus tachycardia are present.[51,65] Importantly, avoid diltiazem and verapamil in young children (especially those under the age of 2 years old) as these agents can cause life-threatening myocardial suppression. For this same reason, although verapamil and diltiazem should be avoided when patients are already on β-adrenoceptor-blocking agents, close monitoring (such as with continuous cardiac monitoring/telemetry) and serial examinations for symptoms of heart failure is strongly advised if patients are being treated with both classes of agents.[65]

6 | CONCLUSION

The foundations of managing paediatric PPGL patients relies upon genetic determinants, pathologic diagnosis, functional imaging analysis, and ultimately, operative intervention requiring commensurate perioperative management. As these fields rapidly advance in the realm of research, critical practice-changing insights must also be translated to clinical practice to afford optimal care.

ACKNOWLEDGEMENTS

This work was supported, in part, by the Intramural Research Programme of the National Institutes of Health, *Eunice Kennedy Shriver* National Institute of Child Health and Human Development and, in part, by the Intramural Research Programme of the Center for Cancer Research, National Cancer Institute.

CONFLICT OF INTEREST STATEMENT

The authors declare no conflict of interest.

ORCID

Matthew A. Nazari http://orcid.org/0000-0002-1956-6077

REFERENCES

1. Choat H, Derrevere K, Knight L, Brown W, Mack EH. SDHB-associated paraganglioma in a pediatric patient and literature review on hereditary pheochromocytoma-paraganglioma syndromes. *Case Rep Endocrinol*. 2014;2014:1-5. doi:10.1155/2014/502734
2. Barontini M, Levin G, Sanso G. Characteristics of pheochromocytoma in a 4- to 20-year-old population. *Ann NY Acad Sci*. 2006;1073(1):30-37. doi:10.1196/annals.1353.003
3. Jochmanova I, Abcede AMT, Guerrero RJS, et al. Clinical characteristics and outcomes of SDHB-related pheochromocytoma and paraganglioma in children and adolescents. *J Cancer Res Clin Oncol*. 2020;146(4):1051-1063. doi:10.1007/s00432-020-03138-5
4. Berends AMA, Buitenwerf E, De Krijger RR, et al. Incidence of pheochromocytoma and sympathetic paraganglioma in the Netherlands: a nationwide study and systematic review. *Eur J Intern Med*. 2018;51:68-73. doi:10.1016/j.ejim.2018.01.015
5. Kuo MJM, Nazari MA, Jha A, Pacak K. Pediatric metastatic pheochromocytoma and paraganglioma: clinical presentation and diagnosis, genetics, and therapeutic approaches. *Front Endocrinol*. 2022;13:936178. doi:10.3389/fendo.2022.936178
6. Pamporaki C, Hamplova B, Peitzsch M, et al. Characteristics of pediatric vs adult pheochromocytomas and paragangliomas. *J Clin Endocrinol Metab*. 2017;102(4):1122-1132. doi:10.1210/jc.2016-3829
7. Bausch B, Wellner U, Bausch D, et al. Long-term prognosis of patients with pediatric pheochromocytoma. *Endocr Relat Cancer*. 2014;21(1):17-25. doi:10.1530/ERC-13-0415
8. Petenuci J, Guimaraes AG, Fagundes GFC, et al. Genetic and clinical aspects of paediatric pheochromocytomas and paragangliomas. *Clin Endocrinol*. 2021;95(1):117-124. doi:10.1111/cen.14467
9. Kittah NE, Gruber LM, Bancos I, et al. Bilateral pheochromocytoma: clinical characteristics, treatment and longitudinal follow-up. *Clin Endocrinol*. 2020;93(3):288-295. doi:10.1111/cen.14222
10. Redlich A, Pamporaki C, Lessel L, Frühwald MC, Vorwerk P, Kuhlen M. Pseudohypoxic pheochromocytomas and paragangliomas dominate in children. *Pediatr Blood Cancer*. 2021;68(7):e28981. doi:10.1002/pbc.28981
11. Park H, Kim MS, Lee J, et al. Clinical presentation and treatment outcomes of children and adolescents with pheochromocytoma and paraganglioma in a single center in Korea. *Front Endocrinol*. 2021;11:610746. doi:10.3389/fendo.2020.610746
12. Roman-Gonzalez A, Zhou S, Ayala-Ramirez M, et al. Impact of surgical resection of the primary tumor on overall survival in patients with metastatic pheochromocytoma or sympathetic paraganglioma.

Ann Surg. 2018;268(1):172-178. doi:10.1097/SLA.0000000000002195
13. Arolfo S, Giraudo G, Franco C, Parasiliti Caprino M, Seno E, Morino M. Minimally invasive adrenalectomy for large pheochromocytoma: not recommendable yet? Results from a single institution case series. *Langenbecks Arch Surg*. 2022;407(1):277-283. doi:10.1007/s00423-021-02312-8
14. Schovanek J, Martucci V, Wesley R, et al. The size of the primary tumor and age at initial diagnosis are independent predictors of the metastatic behavior and survival of patients with SDHB-related pheochromocytoma and paraganglioma: a retrospective cohort study. *BMC Cancer*. 2014;14(1):523. doi:10.1186/1471-2407-14-523
15. Neumann HPH. Distinct clinical features of paraganglioma syndromes associated with SDHB and SDHD gene mutations. *JAMA*. 2004;292(8):943. doi:10.1001/jama.292.8.943
16. Amar L, Bertherat J, Baudin E, et al. Genetic testing in pheochromocytoma or functional paraganglioma. *J Clin Oncol*. 2005;23(34):8812-8818. doi:10.1200/JCO.2005.03.1484
17. Amar L, Baudin E, Burnichon N, et al. Succinate dehydrogenase B gene mutations predict survival in patients with malignant pheochromocytomas or paragangliomas. *J Clin Endocrinol Metab*. 2007;92(10):3822-3828. doi:10.1210/jc.2007-0709
18. Kimura N, Takayanagi R, Takizawa N, et al. Pathological grading for predicting metastasis in phaeochromocytoma and paraganglioma. *Endocr Relat Cancer*. 2014;21(3):405-414. doi:10.1530/ERC-13-0494
19. King KS, Prodanov T, Kantorovich V, et al. Metastatic pheochromocytoma/paraganglioma related to primary tumor development in childhood or adolescence: *SDHB* mutations. *J Clin Oncol*. 2011;29(31):4137-4142. doi:10.1200/JCO.2011.34.6353
20. Lenders JWM, Kerstens MN, Amar L, et al. Genetics, diagnosis, management and future directions of research of phaeochromocytoma and paraganglioma: a position statement and consensus of the Working Group on Endocrine Hypertension of the European Society of Hypertension. *J Hypertens*. 2020;38(8):1443-1456. doi:10.1097/HJH.0000000000002438
21. Scollon S, Anglin AK, Thomas M, Turner JT, Wolfe Schneider K. A comprehensive review of pediatric tumors and associated cancer predisposition syndromes. *J Genet Couns*. 2017;26(3):387-434. doi:10.1007/s10897-017-0077-8
22. Toledo RA, Burnichon N, Cascon A, et al. Consensus statement on next-generation-sequencing-based diagnostic testing of hereditary phaeochromocytomas and paragangliomas. *Nat Rev Endocrinol*. 2017;13(4):233-247. doi:10.1038/nrendo.2016.185
23. Angelousi A, Kassi E, Zografos G, Kaltsas G. Metastatic pheochromocytoma and paraganglioma. *Eur J Clin Invest*. 2015;45(9):986-997. doi:10.1111/eci.12495
24. Havekes B, Romijn JA, Eisenhofer G, Adams K, Pacak K. Update on pediatric pheochromocytoma. *Pediatr Nephrol*. 2009;24(5):943-950. doi:10.1007/s00467-008-0888-9
25. Fishbein L, Leshchiner I, Walter V, et al. Comprehensive molecular characterization of pheochromocytoma and paraganglioma. *Cancer Cell*. 2017;31(2):181-193. doi:10.1016/j.ccell.2017.01.001
26. Pham TH, Moir C, Thompson GB, et al. Pheochromocytoma and paraganglioma in children: a review of medical and surgical management at a tertiary care center. *Pediatrics*. 2006;118(3):1109-1117. doi:10.1542/peds.2005-2299
27. Eisenhofer G, Walther MM, Huynh TT, et al. Pheochromocytomas in von Hippel-Lindau syndrome and multiple endocrine neoplasia type 2 display distinct biochemical and clinical phenotypes. *J Clin Endocrinol Metab*. 2001;86(5):1999-2008. doi:10.1210/jcem.86.5.7496
28. Murgia A, Martella M, Vinanzi C, Polli R, Perilongo G, Opocher G. Somatic mosaicism in von Hippel-Lindau disease. *Hum Mutat*. 2000;15(1):114. doi:10.1002/(SICI)1098-1004(200001)15:1<114::AID-HUMU20>3.0.CO;2-7
29. Druker H, Zelley K, McGee RB, et al. Genetic counselor recommendations for cancer predisposition evaluation and surveillance in the pediatric oncology patient. *Clin Cancer Res*. 2017;23(13):e91-e97. doi:10.1158/1078-0432.CCR-17-0834
30. Raygada M, King KS, Adams KT, Stratakis CA, Pacak K. Counseling patients with succinate dehydrogenase subunit defects: genetics, preventive guidelines, and dealing with uncertainty. *J Pediatr Endocrinol Metab*. 2014;27(9-10):837-844. doi:10.1515/jpem-2013-0369
31. Taïeb D, Hicks RJ, Hindié E, et al. European Association of Nuclear Medicine Guideline/Society of Nuclear Medicine and Molecular Imaging Procedure Standard 2019 for radionuclide imaging of phaeochromocytoma and paraganglioma. *Eur J Nucl Med Mol Imaging*. 2019;46(10):2112-2137. doi:10.1007/s00259-019-04398-1
32. Taïeb D, Jha A, Treglia G, Pacak K. Molecular imaging and radionuclide therapy of pheochromocytoma and paraganglioma in the era of genomic characterization of disease subgroups. *Endocr Relat Cancer*. 2019;26(11):R627-R652. doi:10.1530/ERC-19-0165
33. Taïeb D, Fargette C, Jha A, Pacak K. Nuclear medicine in pheochromocytoma and paraganglioma: at a crossroads with precision medicine. *Endocr Relat Cancer*. 2023;30(4):e220375. doi:10.1530/ERC-22-0375
34. Tella SH, Jha A, Taïeb D, Horvath KA, Pacak K. Comprehensive review of evaluation and management of cardiac paragangliomas. *Heart*. 2020;106(16):1202-1210. doi:10.1136/heartjnl-2020-316540
35. Jha A, Patel M, Carrasquillo JA, et al. Choice is good at times: the emergence of [^{64}Cu]Cu-DOTATATE-based somatostatin receptor imaging in the era of [^{68}Ga]Ga-DOTATATE. *J Nucl Med*. 2022;63(9):1300-1301. doi:10.2967/jnumed.122.264183
36. Jha A, Ling A, Millo C, et al. Superiority of ^{68}Ga-DOTATATE over ^{18}F-FDG and anatomic imaging in the detection of succinate dehydrogenase mutation (SDHx)-related pheochromocytoma and paraganglioma in the pediatric population. *Eur J Nucl Med Mol Imaging*. 2018;45(5):787-797. doi:10.1007/s00259-017-3896-9
37. Nölting S, Bechmann N, Taieb D, et al. Personalized management of pheochromocytoma and paraganglioma. *Endocr Rev*. 2022;43(2):199-239. doi:10.1210/endrev/bnab019
38. States LJ, Reid JR. Whole-body PET/MRI applications in pediatric oncology. *Am J Roentgenol*. 2020;215(3):713-725. doi:10.2214/AJR.19.22677
39. Patel M, Jha A, Ling A, et al. Performances of functional and anatomic imaging modalities in succinate dehydrogenase A-related metastatic pheochromocytoma and paraganglioma. *Cancers*. 2022;14(16):3886. doi:10.3390/cancers14163886
40. Janssen I, Blanchet EM, Adams K, et al. Superiority of [^{68}Ga]-DOTATATE PET/CT to other functional imaging modalities in the localization of *SDHB* -associated metastatic pheochromocytoma and paraganglioma. *Clin Cancer Res*. 2015;21(17):3888-3895. doi:10.1158/1078-0432.CCR-14-2751
41. Janssen I, Chen CC, Millo CM, et al. PET/CT comparing ^{68}Ga-DOTATATE and other radiopharmaceuticals and in comparison with CT/MRI for the localization of sporadic metastatic pheochromocytoma and paraganglioma. *Eur J Nucl Med Mol Imaging*. 2016;43(10):1784-1791. doi:10.1007/s00259-016-3357-x
42. Pang Y, Gupta G, Jha A, et al. Nonmosaic somatic *HIF2A* mutations associated with late onset polycythemia-paraganglioma syndrome: newly recognized subclass of polycythemia-paraganglioma syndrome. *Cancer*. 2019;125(8):1258-1266. doi:10.1002/cncr.31839
43. Han S, Suh CH, Woo S, Kim YJ, Lee JJ. Performance of ^{68}Ga-DOTA-conjugated somatostatin receptor-targeting peptide PET in detection of pheochromocytoma and paraganglioma: a systematic review

and metaanalysis. *J Nucl Med*. 2019;60(3):369-376. doi:10.2967/jnumed.118.211706
44. Taïeb D, Jha A, Guerin C, et al. ^{18}F-FDOPA PET/CT imaging of MAX-related pheochromocytoma. *J Clin Endocrinol Metab*. 2018;103(4):1574-1582. doi:10.1210/jc.2017-02324
45. Janssen I, Chen CC, Zhuang Z, et al. Functional imaging signature of patients presenting with polycythemia/paraganglioma syndromes. *J Nucl Med*. 2017;58(8):1236-1242. doi:10.2967/jnumed.116.187690
46. Jha A, Patel M, Carrasquillo JA, et al. Sporadic primary pheochromocytoma: a prospective intraindividual comparison of six imaging tests (CT, MRI, and PET/CT using ^{68}Ga-DOTATATE, FDG, ^{18}F-FDOPA, and ^{18}F-FDA). *Am J Roentgenol*. 2022;218(2):342-350. doi:10.2214/AJR.21.26071
47. Jha A, Taïeb D, Carrasquillo JA, et al. High-specific-activity-^{131}I-MIBG versus ^{177}Lu-DOTATATE targeted radionuclide therapy for metastatic pheochromocytoma and paraganglioma. *Clin Cancer Res*. 2021;27(11):2989-2995. doi:10.1158/1078-0432.CCR-20-3703
48. Carrasquillo JA, Chen CC, Jha A, Pacak K, Pryma DA, Lin FI. Systemic radiopharmaceutical therapy of pheochromocytoma and paraganglioma. *J Nucl Med*. 2021;62(9):1192-1199. doi:10.2967/jnumed.120.259697
49. Flynn JT, Kaelber DC, Baker-Smith CM, et al. Clinical practice guideline for screening and management of high blood pressure in children and adolescents. *Pediatrics*. 2017;140(3):e20171904. doi:10.1542/peds.2017-1904
50. Wolf KI, Santos JRU, Pacak K. Why take the risk? We only live once: the dangers associated with neglecting a pre-operative alpha adrenoceptor blockade in pheochromocytoma patients. *Endocr Pract*. 2019;25(1):106-108. doi:10.4158/EP-2018-0455
51. Nazari MA, Rosenblum JS, Haigney MC, Rosing DR, Pacak K. Pathophysiology and acute management of tachyarrhythmias in pheochromocytoma. *J Am Coll Cardiol*. 2020;76(4):451-464. doi:10.1016/j.jacc.2020.04.080
52. Eisenhofer G, Prejbisz A, Peitzsch M, et al. Biochemical diagnosis of chromaffin cell tumors in patients at high and low risk of disease: plasma versus urinary free or deconjugated O-methylated catecholamine metabolites. *Clin Chem*. 2018;64(11):1646-1656. doi:10.1373/clinchem.2018.291369
53. Finnerty FA, Buchholz JH, Guillaudeu RL. The blood volumes and plasma protein during levarterenol-induced hypertension. *J Clin Invest*. 1958;37(3):425-429. doi:10.1172/JCI103622
54. Brock L. Hypovolaemia and phaeochromocytoma. *Ann R Coll Surg Engl*. 1975;56(4):218-221.
55. Stenström G, Kutti J. The blood volume in pheochromocytoma patients before and during treatment with phenoxybenzamine. *Acta Med Scand*. 2009;218(4):381-387. doi:10.1111/j.0954-6820.1985.tb08862.x
56. Glass AR. Pheochromocytoma, prazosin, and hypotension. *Ann Intern Med*. 1982;97(3):455. doi:10.7326/0003-4819-97-3-455_2
57. Pacak K. Preoperative management of the pheochromocytoma patient. *J Clin Endocrinol Metab*. 2007;92(11):4069-4079. doi:10.1210/jc.2007-1720
58. Batisse-Lignier M, Pereira B, Motreff P, et al. Acute and chronic pheochromocytoma-induced cardiomyopathies: different prognoses? A systematic analytical review. *Medicine*. 2015;94(50):e2198. doi:10.1097/MD.0000000000002198
59. Paur H, Wright PT, Sikkel MB, et al. High levels of circulating epinephrine trigger apical cardiodepression in a β_2-adrenergic receptor/G_i-dependent manner: a new model of takotsubo cardiomyopathy. *Circulation*. 2012;126(6):697-706. doi:10.1161/CIRCULATIONAHA.112.111591
60. Gagnon N, Mansour S, Bitton Y, Bourdeau I. Takotsubo-like cardiomyopathy in a large cohort of patients with pheochromocytoma and paraganglioma. *Endocr Pract*. 2017;23(10):1178-1192. doi:10.4158/EP171930.OR
61. Riester A, Weismann D, Quinkler M, et al. Life-threatening events in patients with pheochromocytoma. *Eur J Endocrinol*. 2015;173(6):757-764. doi:10.1530/EJE-15-0483
62. Mamilla D, Araque K, Brofferio A, et al. Postoperative management in patients with pheochromocytoma and paraganglioma. *Cancers*. 2019;11(7):936. doi:10.3390/cancers11070936
63. Nisticò D, Bossini B, Benvenuto S, Pellegrin MC, Tornese G. Pediatric adrenal insufficiency: challenges and solutions. *Ther Clin Risk Manag*. 2022;18:47-60. doi:10.2147/TCRM.S294065
64. Jaiswal SK, Memon SS, Lila A, et al. Preoperative amlodipine is efficacious in preventing intraoperative HDI in pheochromocytoma: pilot RCT. *J Clin Endocrino Metab*. 2021;106(8):e2907-e2918. doi:10.1210/clinem/dgab231
65. Flynn JT, Pasko DA. Calcium channel blockers: pharmacology and place in therapy of pediatric hypertension. *Pediatr Nephrol*. 2000;15(3):302-316. doi:10.1007/s004670000480

How to cite this article: Nazari MA, Jha A, Kuo MJM, et al. Paediatric phaeochromocytoma and paraganglioma: a clinical update. *Clin Endocrinol (Oxf)*. 2024;101:446-454. doi:10.1111/cen.14955